Endocrine (2011) 40:41–54
DOI 10.1007/s12020-011-9438-5

ORIGINAL ARTICLE

Preimplantation factor (PIF) analog prevents type I diabetes mellitus (TIDM) development by preserving pancreatic function in NOD mice

Lola Weiss · Steve Bernstein · Richard Jones · Ravi Amunugama · David Krizman · Lellean JeBailey · Osnat Hazan · Janna Yachtin · Reut Shiner · Israel Reibstein · Elizabeth Triche · Shimon Slavin · Reuven Or · Eytan R. Barnea

Received: 27 January 2011 / Accepted: 31 January 2011 / Published online: 22 March 2011

Abstract Preimplantation factor (PIF) is a novel embryo-secreted immunomodulatory peptide. Its synthetic analog (sPIF) modulates maternal immunity without suppression. There is an urgent need to develop agents that could prevent the development of type 1 diabetes mellitus (TIDM). Herein, we examine sPIF's preventive effect on TIDM development by using acute adoptive-transfer (ATDM) and spontaneously developing (SDM) in non-obese diabetic (NOD) murine models. Diabetes was evaluated by urinary and plasma glucose, intraperitoneal glucose tolerance test (IPGTT), pancreatic islets insulin staining by immunohistochemistry and by pancreatic proteome evaluation using mass spectrometry, followed by signal pathway analysis. Continuous administration of sPIF for 4-weeks prevents diabetes development in ATDM model in >90% of recipients demonstrated by normal IPGTT, preserved islets architecture, number, and insulin staining. ($P < 0.01$). sPIF effect was specific; its protective effects are not replicated by scrambled PIF ($\chi^2 = 0.009$) control. sPIF led also to increased circulating Th2 and Th1 cytokines. In SDM model, 4-week continuous sPIF administration prevented onset of diabetes for 21 weeks post-therapy ($P < 0.01$). Low-dose sPIF administration for 16 weeks prevented diabetes development up to 14 weeks post-therapy, evidenced by preserved islets architecture and insulin staining. In SDM model, pancreatic proteome pathway analysis demonstrated that sPIF regulates protein traffic, prevents protein misfolding and aggregation, and reduces oxidative stress and islets apoptosis, leading to preserved insulin

Electronic supplementary material The online version of this article (doi:10.1007/s12020-011-9438-5) contains supplementary material, which is available to authorized users.

L. Weiss · O. Hazan · J. Yachtin · R. Shiner · I. Reibstein · R. Or
Department of Bone Marrow Transplantation and Cancer Immunotherapy, Hadassah University Hospital Ein Kerem, Hebrew University, Jerusalem, Israel

S. Bernstein
QualTek Molecular Laboratories, Santa Barbara, CA, USA

R. Jones · R. Amunugama
NextGen Sciences Ltd., Ann Arbor, MI, USA

D. Krizman
Expression Pathology, Inc., Gaithersburg, MD, USA

L. JeBailey
GeneGo Inc., St. Joseph, MI, USA

S. Slavin
International Center for Cell Therapy & Cancer Immunotherapy (CTCI), Tel Aviv, Israel

E. Triche
Department of Community Health and Epidemiology, Brown University School of Medicine, Providence, RI, USA

E. R. Barnea (✉)
The Society for the Investigation of Early Pregnancy (SIEP), 1697 Lark Lane, Cherry Hill, NJ 08003, USA
e-mail: barnea@earlypregnancy.org

E. R. Barnea
Department of Obstetrics and Gynecology, University of Medicine and Dentistry of New Jersey, Robert Wood Johnson Medical School, Camden, NJ, USA

staining. sPIF further increased insulin receptor expression and reduced actin and tubulin proteins, thereby blocking neutrophil invasion and inflammation. Exocrine pancreatic function was also preserved. sPIF administration results in marked prevention of spontaneous and induced adoptive-transfer diabetes suggesting its potential effectiveness in treating early-stage TIDM.

Keywords TIDM · Preimplantation factor · Therapy · Pancreas · NOD

Introduction

Insulin-dependent type 1 (juvenile) diabetes (TIDM) leads to destruction of insulin-producing pancreatic islet beta cells causing a life-long dependence on insulin administration. The etiology of TIDM is complex and involves a combination of genetic, environmental, and immunological influences [1, 2]. TIDM is characterized by a progressive, asymptomatic decline in beta-cell function until hyperglycemia develops [3]. The disease process begins with infiltration of mononuclear cells around the islets and proceeds with destruction of the insulin-producing beta cells [4]. Islet destruction is mediated by $CD4^+$ and $CD8^+$ T cells, activated by specific pancreatic antigens [5]. In fulminant TIDM, macrophage infiltration dominates coupled with increased expression of TOLL receptors. The important role of protein misfolding and oxidative stress leading to islet cells apoptosis in TIDM was also documented [6].

Currently used TIDM preventive measures are suboptimal. Insulin is needed to control glucose levels and more rarely islet transplantation is carried out [7]. In addition, immune therapies by using antibodies (anti-CD3 and anti-thymocyte globulin) to block the autoimmune cascade [8, 9] combined with agents that repair or regenerate beta cells (e.g., glulisine, glucagon-like-peptide-1 (GLP-1), extendin-4, and Dia-Pep277) were tested. Also, more recently non-myeloablative allogenic bone marrow transplantation and heparanase were tested with variable success [8–13]. In TIDM total islet destruction does not frequently occur. However, despite that insulin production is severely curtailed. Thus, an ideal therapy for early-stage diabetes should prevent total islet destruction and also reactivate islet stem cells leading to their differentiation into insulin producing cells [14].

In this study we draw lessons from mammalian pregnancy, where the resulting unique altered immune milieu benefits both mother and fetus/semi-total allograft. Interestingly, pregnancy often leads to attenuation of several autoimmune disorders [15, 16] to frequently flare up postpartum. Thus, pregnancy-specific protective mechanisms are operative, albeit temporarily involving complex but not fully elucidated mechanisms. In pregnancy, there is a unique compensatory increase in pancreatic beta-cells proliferation, counterbalancing for the excess metabolic burden due to presence of the placenta and fetus [17, 18].

The Barnea Group has isolated a peptide from embryo culture media and determined its sequence [19]. We reported that viable embryos secrete this novel peptide named, pre-implantation factor (PIF, 15 aa) [20–25] present in maternal circulation, expressed by the placenta. PIF plays a significant role in creating/maintaining maternal immune tolerance without suppression [22]. We demonstrated that in women PIF displays essential multi-targeted effects, of regulating immunity, promoting embryo-decidual adhesion, and controlling adaptive apoptotic processes in the decidua [26]. In addition, PIF promotes trophoblast invasion thus facilitating placental development, furthering maternal acceptance of the embryo [27]. Hence, if PIF could prevent the observed targeted immune attack on the pancreas in TIDM disease management could be greatly improved.

Since PIF has immune modulatory properties; herein we investigate the synthetic version of PIF (sPIF) effectiveness in preventing TIDM by preserving islet function using the NOD mouse model which is frequently used to test novel therapies against TIDM [8–13]. In this model in females by 12 weeks start to develop diabetes and by 18–20 weeks 90% of them become diabetic. In contrast, male NOD mice develop spontaneously DM only in 10% [11, 12]. To address the principal etiologies that lead to TIDM development, we examined sPIF's efficacy in two relevant NOD models, adoptive-transfer (rapidly immune-induced) and in spontaneously developing mice. Diabetes development was monitored by urinary and plasma glucose, IPGTT, pancreas histology, peripheral cytokines, and proteome evaluation. Data generated is relevant for management of early-stage TIDM.

Results

Continuous 4-week sPIF administration protects long-term against DM in an adoptive-transfer model (ATDM)

In this mouse model insulinopenia is rapidly produced [11]. Diabetes was induced in male NOD recipients by infusion of splenocytes derived from diabetic female NOD mice. Subsequently, they were administered sPIF (0.83 or 2.73 mg/kg/day/28 days), or PBS (control) via a subcutaneously implanted Alzet pump and followed for 40 days post-therapy. Diabetes development was documented by urine glucose levels (>250 mg/dl) and plasma glucose levels

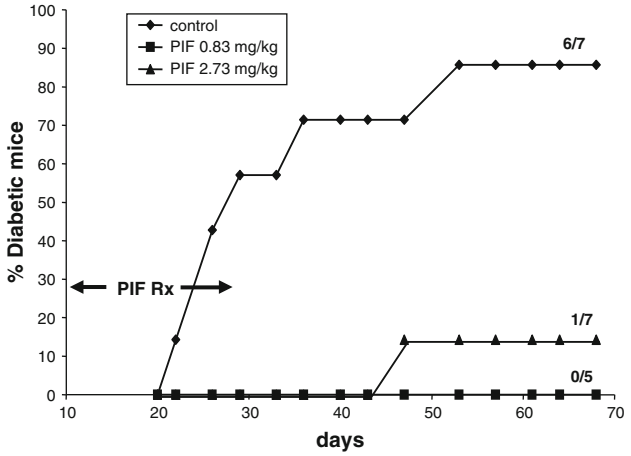

Fig. 1 sPIF administration prevents TIDM in NOD adoptive-transfer male murine model (ATDM). Male mice were injected intravenously with 25 million spleen cells derived from diabetic female NOD mice. sPIF (0.83 or 2.73 mg/kg/day) or PBS (control) was administered using an Alzet pump for 28 days, followed by 40-day observation period. In the low-dose sPIF-treated group, no mice developed diabetes, while in the high-dose treated group, one mouse became diabetic. In contrast, in PBS-treated mice 6/7 became diabetic ($P = 0.001$) versus both PIF treatment groups

tested at 60 min after IPGTT day 60, and at 40 days post-therapy. In the combined sPIF-treated groups, only one (1/12) mouse developed diabetes, compared with (6/7) in control mice (χ^2, $P = 0.003$) (Fig. 1). Moreover in the control group (2/7) had >600 mg/dl glucose levels versus none in the combined sPIF-treated groups. (χ^2, $P = 0.05$). Table 1 shows individual mice's circulating glucose levels. In controls most mice were diabetic by 40 days; some having >600 mg/dl plasma glucose levels. Moreover, post-IPGTT 5/6 and 4/6 mice at the higher and lower sPIF dose, respectively, had a normal IPGTT versus 0/7 in controls, (χ^2, $P = 0.01$). In a confirmatory experiment, an intermediate sPIF dose (1.03 mg/kg/day/for 4 weeks using an Alzet pump) was used. Until day 35, only 1/8 of the sPIF-treated mice developed diabetes, compared to 3/4 of controls (χ^2, $P = 0.03$). Mice that were followed up to 70 days also showed a significant PIF-induced protection, Mann–Whitney ($P = 0.03$). This indicated that higher continuous sPIF doses are not more effective than the lowest dose used.

Low-dose subcutaneous sPIF injections protect against DM development in ATDM clinically relevant model

Since subcutaneous injections are easier to administer, we tested in ATDM model sPIF (0.08 or 0.16 mg/kg twice daily, 5/day a week until day 28), at doses ~5–10 times lower than used in the Alzet experiments and compared with PBS or

Table 1 sPIF prevents DM development in NOD murine model as determined by blood glucose levels

Treatment	Mice	Glucose levels (mg/dl) at day 40	Glucose levels (mg/dl) at day 69	IPGTT glucose levels at 60 min (mg/dl)
sPIF (0.83 mg/kg/day)	#1	131	97	131
	#2	112	106	171
	#3	137	119	222
	#4	132	109	190
	#5	130	149	290
	Mean ± SE	128.4 ± 2.3	116 ± 8.6	200 ± 26
sPIF (2.73 mg/kg/day)	#1	118	87	151
	#2	126	108	135
	#3	125	111	150
	#4	113	144	187
	#5	158	514	–
	#6	123	103	191
	#7	115	109	256
	Mean ± SE	125.4 ± 3.9	168 ± 40.2	178 ± 18
Control (PBS)	#1	>600	355	–
	#2	>600	377	–
	#3	202	230	–
	#4	191	Dead	–
	#5	>600	Dead	–
	#6	298	207	–
	#7	135	123	204
	Mean ± SE	375 ± 56.5	258.4 ± 42.4	

sPIF therapy prevented development of DM in 11/12 treated versus 6/7 in control mice. Time course of DM development is seen in Fig. 1. Blood samples were collected by venipuncture and glucose levels were measured by glucose oxidase method, using an automatic analyzer. IPGTT was determined by injecting glucose IP 1 gm/kg, and collecting blood sample 1 h later. Abnormal IPGTT result was considered >160 mg/dl glucose level

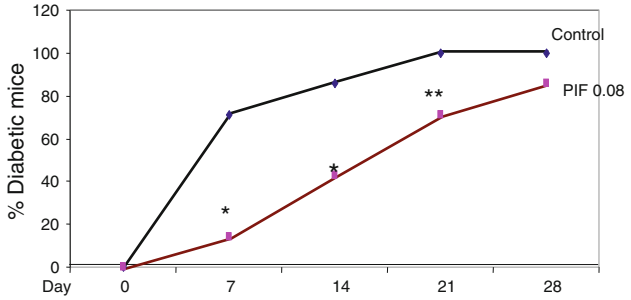

Fig. 2 Low-dose sPIF injections protect against diabetes development in ATDM model. sPIF 0.08 mg/kg ×2 day injections (5 consecutive days/week) were administered and mice were followed by twice weekly urinary glucose measurements. sPIF treatment protected against DM treatment versus controls until day 24, χ^2, $P = 0.04$

naïve controls. The lower sPIF dose led to significant protection versus combined controls until day 24, χ^2, $P = 0.04$ (Fig. 2) (n = 7–8/group). At the higher dose the protection was similar but it did not reach statistical significance, $P < 0.058$ (not shown). Thus, sPIF at very low doses is also effective against TIDM development.

sPIF effect is specific and replicated by scrambled PIF

Since protection was not total in the subcutaneous low dose tested, we have examined also a higher sPIF dose as well. Further to determine sPIF specificity sPIF effect was compared with scrambled PIFscr (same amino acids as sPIF but in random order). Mice were injected with sPIF 0.75 mg/kg ×2/day or PIFscr 0.75 mg/kg ×2/day ($n = 5$/group) daily for 15 days monitoring serially plasma glucose measurements (Fig. 3)**.** Results showed that none of the sPIF mice (0/5) developed diabetes while 4/5 of the PIFscr treated mice had diabetes, which was already evident by the observed hyperglycemia shortly after disease induction χ^2, $P = 0.009$. We have analyzed a number of cytokines Th1, and Th2 secreted by isolated splenocytes from these mice after 72 h of culture finding no differences between the two groups. On the other hand, we found an increase in a number of circulating cytokines, IL1a, IL2, IL5, and IL6, in all cases $P < 0.05$, Mann–Whitney in the sPIF-treated group versus PIFscr. This result implies that sPIF-induced protection is specific and is not replicated by a scrambled PIF and this protection is associated with changes with circulating immune markers.

sPIF administration protects against insulinitis development

The sPIF-treated pancreatic islets architecture was examined by immunohistochemistry (Data from Fig. 1). sPIF protected against islet destruction: architecture was intact,

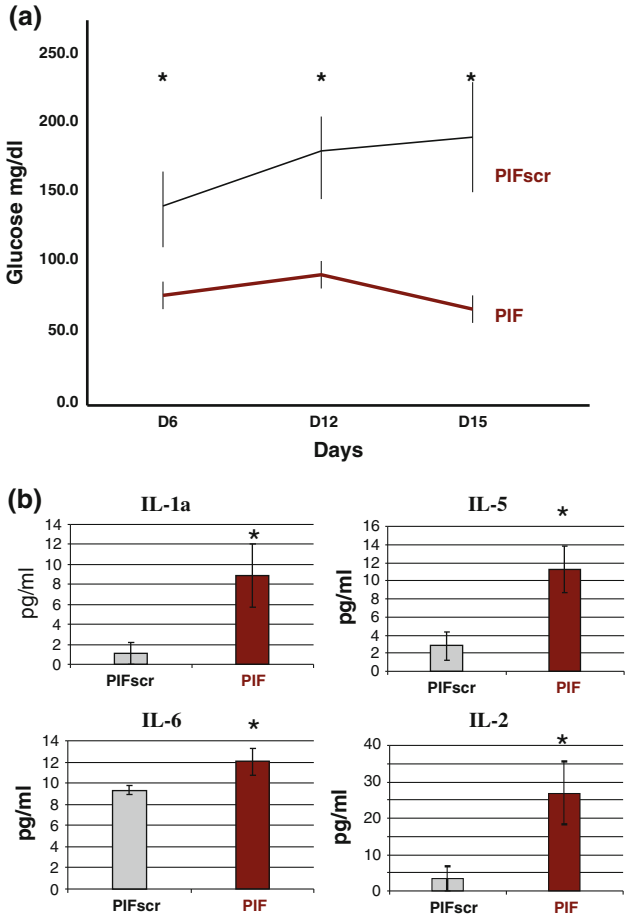

Fig. 3 sPIF effect not replicated by scrambled PIF in ATDM model-changes in cytokines. Mice were injected with sPIF or PIFscr and diabetes development was monitored by serially testing plasma glucose levels, and determining Th1 and Th2 cytokine levels. **a** All sPIF-treated mice ($n = 5$) glucose levels were normal throughout the experiment. In contrast 4/5 of PIFscr treated mice developed persistent hyperglycemia. χ^2, $P = 0.009$. **b** Levels of IL6 were higher, $P < 0.047$, Levels of IL 5 were higher, $P = 0.03$, Levels of IL2 were higher $P = 0.047$, levels of IL1a were higher $P = 0.047$, all cytokines versus PIFscr, Mann–Whitney

insulin staining was intense, and surrounding inflammatory cells numbers were reduced and did not penetrate into the islets. In contrast, in PBS-treated mice (control) islet architecture was distorted, islet number was reduced, insulin staining was minimal and significant numbers of inflammatory cells penetrated the pancreatic islets, (Fig. 4a–c). sPIF's observed effect was significant: number of islets present (ANOVA $P = 0.01$) and intensity of staining which was six- to sevenfold higher than the control (non-parametric, Mann–Whitney $P = 0.01$). $N = 4$/group (Fig. 4d, e). As an additional control we have also compared sPIF effect on islets histology with a group of naïve non-diabetic male mice matched for age ($N = 6$). We found that islet scoring in the naïve mice was significantly

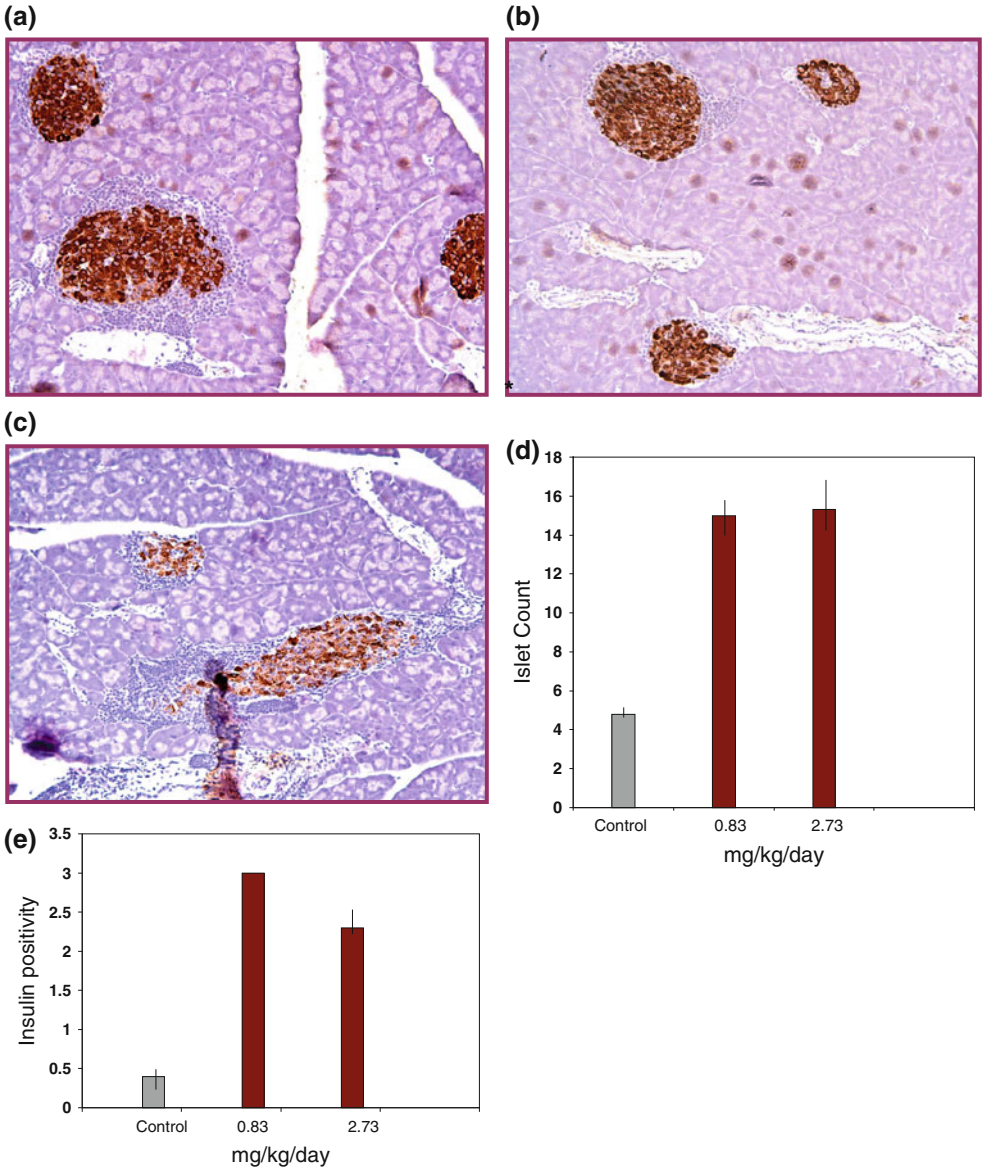

Fig. 4 sPIF administration preserves insulin and islets architecture in adoptive-transfer NOD model. Mice treated (Fig. 1) were euthanized and pancreatic tissue evaluated by using anti-insulin antibody to document insulin staining and islet number within the pancreas. In addition, the extent of inflammatory cells infiltration was evaluated. The pictograph (representative) demonstrates intact pancreatic islets in sPIF-treated mice with low surrounding inflammation (**a**, **b**) versus control (**c**) where massive islet inflammation coupled with reduced islet number and insulin intensity was noted. **d** Shows that sPIF treatment leads to islet number preservation versus controls, $P = 0.01$. **e** Demonstrates that PIF treatment preserved insulin staining positivity, seven-fold higher than controls, where staining was minimal. (Mann–Whitney $P = 0.01$) $N = 4$/group

higher than the sPIF-treated mice Mean ± SEM 36.5 ± 1.8 vs. 15 ± 2, $P < 0.001$, respectively.

Short-term sPIF administration prevents spontaneous DM (SDM) long-term post-therapy

In the first long-term experiment, sPIF was administered (0.68 or 2.5 mg/kg/day/28 days) or PBS, (by Alzet pump) to 6–7 weeks-old female NOD mice. Mice were monitored by urinary glucose twice weekly for upto 35 weeks, 21 weeks post-therapy. The higher sPIF treatment protected against diabetes development as analyzed by the percent of diabetic mice development at each time period (non-parametric Mann–Whitney, $P = 0.03$), area under the curve versus controls. (Fig. 5). At the higher sPIF dose 4/8 mice remained diabetes free until 30 weeks, for 16 weeks post-therapy while only 1/7 at the lower dose and in 2/7 of controls. The low-dose sPIF effect was similar to controls

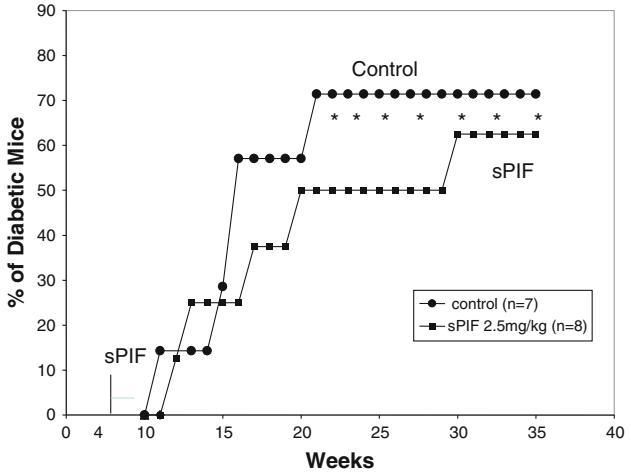

Fig. 5 Short-term sPIF prevents TIDM long-term post-therapy in female NOD mice. Mice were implanted subcutaneously (Alzet pump 0.68 or 2.5 mg/kg/day/28 day) or PBS and followed for 21 weeks post-therapy. The higher sPIF dose protected against diabetes development, (Mann–Whitney $P = 0.03$), versus PBS. The protective effect of the higher dose lasted until the end of the observation period. The lower sPIF dose effect was similar to controls (not shown)

(Mann–Whitney = NS). We show that short-term sPIF treatment prevented TIDM long term.

Low-dose sPIF subcutaneous injections prevent long-term SDM

Since DM is a chronic condition we aimed to examine sPIF administration in a realistic model of clinical management. Female mice at 5–6 weeks of age were injected five-times/week with very low doses (0.075 or 0.15 mg/kg/day, similarly to doses used in ATDM) sPIF (12–30-fold lower than the effective dose, 2.5 mg/kg/day) or PBS or control ($N = 12$/total) for 16 weeks followed by 14 weeks post-therapy. In control mice 6/12 developed diabetes by 20 weeks vs. 0/5 in the high sPIF dose (χ^2, $P < 0.05$), 4 weeks post-therapy. The lower dose sPIF was effective until 26 weeks, ($P < 0.03$, Mann–Whitney) area under the curve. At 30 weeks, 3/6 at the lower and (2/5, one latent) at the higher dose treated mice remained free of DM. These results confirmed long-term TIDM prevention post-therapy in a clinical realistic setting.

sPIF preserves long-term islets architecture and insulin staining in SDM

Pancreatic islets were examined following long-term low-dose sPIF administration in SDM. sPIF treatment preserved islet architecture, number and insulin staining intensity. In contrast, control mice showed complete islet destruction and minimal insulin staining. Islets histological features are summarized in Table 2 and Fig. 6a–d. Thus sPIF preserved pancreatic histological features in a similar manner as observed in ATDM.

sPIF preserves pancreatic function: proteome analysis

Mouse pancreatic proteome was examined following subcutaneously injected low sPIF doses in SDM 14 weeks post-therapy. Using direct mass spectrometry, we determined sPIF-to-control ratio of evaluable pancreatic proteins of >200 of the total pancreas. Table 3 lists certain mechanistically relevant proteins whose expression was significantly changed as analyzed by ANOVA followed by two tailed *t*-test ($P < 0.05$). The profile of the two sPIF-treated healthy mice was as expected, similar (Table 2). sPIF reduced proteins of the pro-inflammatory group related to mast cell and macrophage function, that block inflammatory cytokines (tumor necrosis factor α (TNF-α) (Chi3L3), those involved in inflammatory cells function (KRT8, 18). sPIF further reduced proteins that promote apoptosis (HNMPa2b1, RPs10). In contrast, sPIF promoted insulin processing and receptor function (HSP90B1, PDEA2), and pancreatic exocrine function (COL1A1, AMY2A). Overall, proteome analysis reveals a dual protective effect lower inflammation and enhanced exocrine function.

Table 2 sPIF preserves long-term insulin expression in female NOD murine model prone to develop DM

Treatment	H&E	Insulin
Control ($N = 4$)	Atrophied-islets	0
sPIF		
0.075	Preserved islets structure/number—ductal Inflammation	+++
0.075	Preserved islets structure/number—ductal Inflammation	+++
0.075	Preserved islet structure/number—no Inflammation	+++
0.15	Preserved islet structure/number—ductal Inflammation	+++

Low-dose sPIF (0.075 or 0.15 mg/kg/5 days/week for 16 weeks) was administered subcutaneously to female NOD mice followed by 14 weeks post-therapy

Figure 4 shows individual mice histology and insulin staining

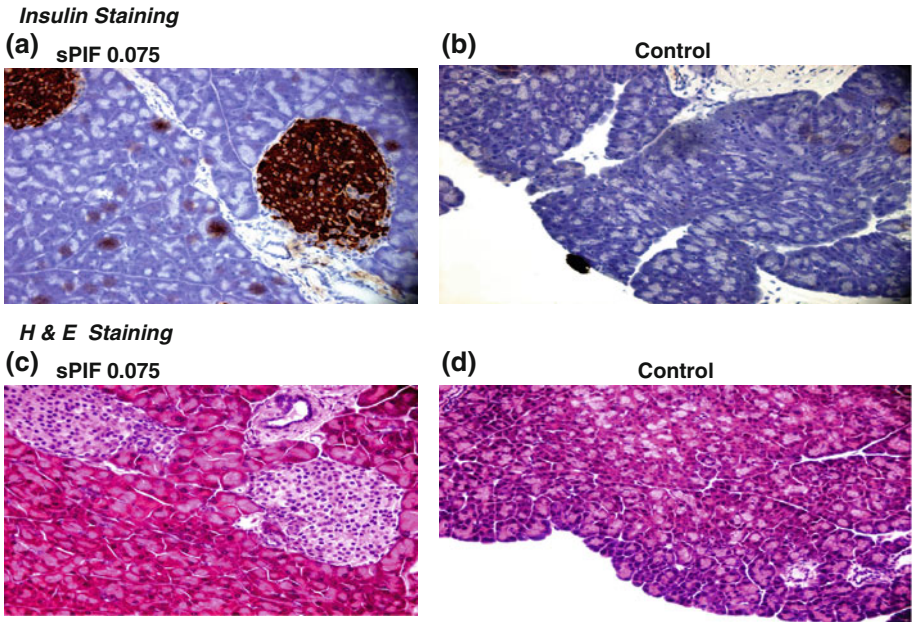

Fig. 6 Low-dose sPIF preserves insulin production and islet cells architecture long–term after treatment ends. Female NOD mice were injected for 16 weeks with sPIF 0.075, or 0.15 mg/kg/days/5 days/week or PBS and followed for 14 weeks post-therapy. The 0.075 PIF-treated group preserved islets architecture and insulin staining, compared to control ($N = 4$) where diffuse atrophy was noted. Table 2 details the histological findings. **a** Demonstrates preserved insulin staining in sPIF-treated mice versus (control) (**b**), where insulin is absent. **c** Demonstrates preserved sPIF islets architecture without inflammatory cells penetration, while (**d**) control, islets were practically absent

Holistic proteome pathway sPIF analysis

A more holistic approach was applied to characterize differences in proteomics results. The most representative functions and pathways were determined using GeneGo's MetaCore suite 6.0 by parsing the data across several ontologies. Results for the diabetic and the sPIF-treated healthy mice represent different stages of protein translation, folding, changes in cytoskeleton remodeling and cell adhesion (Fig. 6 GG processes and GO histograms). sPIF increased expression of elongation factors and decreased RPS/RPL proteins suggesting a shift to increased protein elongation, rather than initiation of translation. Mechanisms involved in protein traffic specifically in response to an accumulation of unfolded proteins is also highly represented (Fig. 7). For instance HSP90B1, GRP78 and Endoplasmin are elevated contributing to protein traffic and regulation of apoptosis. sPIF also induces the expression of PDIa2, P4HB, and VCP, which catalyze protein folding, inhibit aggregation and promote vesicle traffic, respectively. ERO1 and HYOU are known mediators of protein folding in the ER specifically under oxidative stress, and are also elevated with sPIF (Fig. 8, shows the unfolded protein network). Collectively these results demonstrate that low dose sPIF may reverse the ER-stress that occurs at the molecular level of DM. Proteins that were reduced include actin, tubulins, and myosin and may be indicative of a decrease in inflammatory response reducing the need for dynamic actin remodeling required for neutrophil invasion.

Discussion

The present study demonstrates that short-term sPIF, an embryo-secreted, synthetically produced peptide with immune-modulatory properties, can prevent TIDM onset long-term. sPIF effectiveness was demonstrated in both adoptive-transfer (ATDM) and spontaneous NOD (SDM) models, covering realistic disease scenarios. In both models islet architecture and insulin staining was preserved. We also demonstrated that sPIF protective effect is specific and is not replicated by scrambled PIF. sPIF reduced local inflammation, protein misfolding and oxidative stress proteins while promoting insulin processing and exocrine pancreas function. The use of these two models is particularly relevant since TIDM develops in patients with susceptible genotype where the condition is activated by an adverse environmental exposure [4].

In ATDM, short-term continuous sPIF administration prevented diabetes development for several weeks post-therapy documented by IPGTT and confirmed by pancreas histology. Nearly all sPIF-treated mice did not develop diabetes and mean circulating glucose levels were

Table 3 sPIF maintains insulin expression and exocrine pancreas function by reducing inflammatory elements in susceptible female NOD murine model

Name	Islet cells function	Accession numbers	sPIF 0.075 (%)	sPIF 0.075 $P <$	sPIF 0.15 (%)	sPIF 0.15 $P <$
PDIA2	Protein disulfide isomerase assoc. 2	IPI347894, IPI880560	132	0.011	156	0.005
PDI6	Protein disulfide isomerase assoc. 6	IPI854971	220	0.072	340	0.007
P4HB	Propyl-hydroxylase 4 beta	IPI122815	196	0.005	163	0.001
HSP90B1	Heat shock protein 90b1	IPI129526	255	0.001	200	0.01
Ac02	Aconitate hydratase, mitochondrial	IPI116074	300	0.003	0	0.990
ALDH6A1	Methylmalonate-semialdehyde dehydrogen 6A1	IPI461964	400	0.001	266	0.001
ACTB	Actin, cytoplasmic 1	IPI10850, IPI652436	−58	0.000	−50	0.002
EEF1B2	Elongation factor 1b	IPI320208	267	0.008	166	0.1
Control of inflammation						
Hnrnpa2b1	Hetero. ribonucleoprot. iso3	IPI405058, IPI622847	−71	0.012	−43	0.125
Rps10	40S ribosomal protein S10	IPI112448	−91	0.001	−18	0.058
Chi3L3	Chitinase-3 like-3	IP1157508	−99	0.001	−99	0.001
KRT8	Keratin, II cytoskeletal 8	IPI322209	147	0.046	200	0.002
KRT18	Keratin, I cytoskeletal 18	IPI311493	311	0.01	233	0.064
ELA3A	Elastase 3B	IPI132043	−57	0.032	−57	0.045
CPA1	Carboxypeptidase A1	IPI356448	−65	0.001	−43	0.004
FTL1	Ferritin light chain 1	IPI608020, IPI762203	−99	0.001	−99	0.001
Exocrine pancreas						
AMY2A	Amylase 2	IPI756078	200	0.003	215	0.003
CTRB1	Chymotrypsinogen B	IPI315696	−51	0.004	−35	0.016
COL1A1	Collagen alpha-1(I) chain iso.	IPI329872, IPI623191	−83	0.004	−99	0.001

NOD mice treated with sPIF 0.075 or 0.15 mg/kg/day SC for 16 weeks followed by 14 weeks of observation were euthanized and their pancreas was compared to a PBS-treated control mouse. Extracted pancreas (see methods) proteins were examined by mass spectrometry determining in triplicate percent change from control and related statistical significance

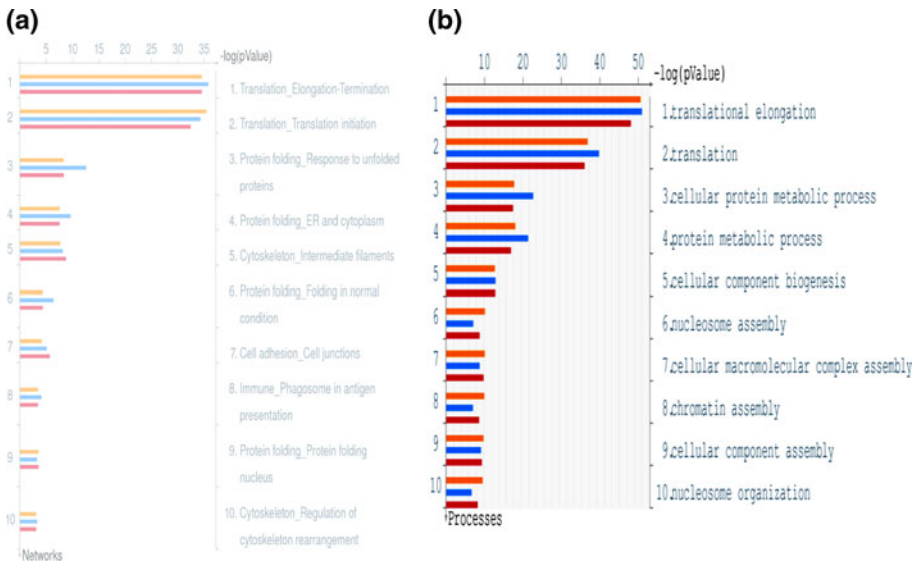

Fig. 7 Enrichment analyses of mass apectroscopy results with metacore 6.0. The top 10 most representative functions from the proteomics results from diabetic mice (*orange*), 0.075 mg sPIF (*blue*) and 0.15 mg sPIF (*red*) are shown across two ontologies: GeneGo Process Networks (**a**) and Gene Ontology (**b**). The results are ordered by −log10 of the p-value of the hypergeometric distribution. This data is highly representative of changes in protein translation according to both ontologies. GeneGo process Networks ontology further describes representation of protein folding response to accumulation of unfolded proteins, changes in the cytoskeleton and cell adhesion (Color figure online)

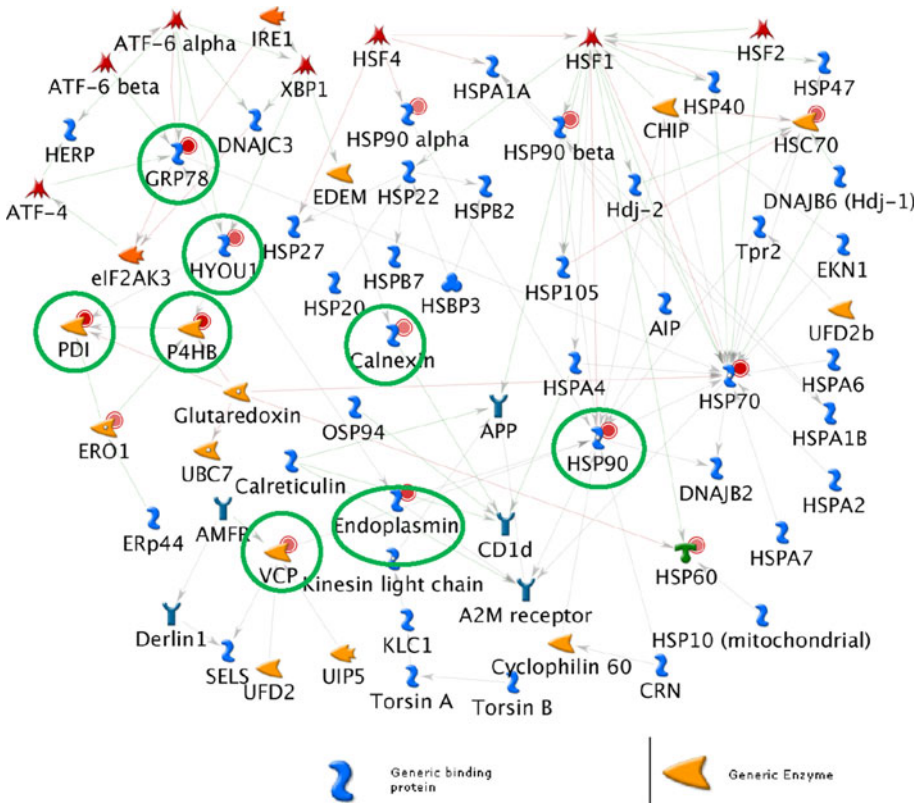

Fig. 8 Representation of the protein folding response to unfolded proteins network by GeneGo* ontology. Shown is the pre-built network that describes the elements of protein folding, specifically in response to protein folding. Relationship between two items are indicated by a *colored arrow* (*green* = positive effect, *red* = negative effect). The proteomics data is overlaid, and proteins from the data are marked with *circles* in the upper right hand corner of each object. Low-dose sPIF induced the expression of several proteins known to alleviate the stress of proteins accumulating in the ER (*circles in green*) (Color figure online)

three-fold lower than in controls. Pancreas histology confirmed that sPIF maintains insulin expression. Since inflammatory cells access to the organ and islets was minimized, a "benign insulinitis" was noted where both islet integrity and insulin staining intensity were preserved as compared with controls. Thus sPIF may lead to islet regeneration, or at least less destruction, by preserving the islets' membrane integrity which did not appear to be violated.

Subcutaneously injected sPIF, at substantially lower doses than used with Alzet pumps equally prevented diabetes development. This minimally invasive method and sPIF dose could facilitate eventual clinical application. sPIF's anti-diabetic effect appears to be physiological and not pharmacological in accord with our recent data generated in other immune models [26].

To demonstrate sPIF specificity the effect of the peptide was compared with a scrambled PIF (same amino acids but in different order). The data demonstrated that all sPIF-treated mice remained disease free while the majority of mice treated with the scrambled peptide became hyperglycemic. This confirmed that sPIF effect is specific and is not replicated by a control peptide. Changes in some circulating cytokines were found at the end of the experiment with increases on both Th1 and Th2 cytokine such as IL5 was observed. Particularly relevant is the increase noted in circulating IL6 known to decrease insulin resistance. This cytokine was recently demonstrated to be relevant in blocking diabetes development by mesenchimal stem cells predominantly through an IL-6-dependent mechanism [28]. The role of other cytokines especially Th2 type shown to be increased by sPIF may aid in minimizing peripheral inflammation. On the other hand PIF did not affect splenocytes cytokine in secretion, which may point to a more targeted combined anti-inflammatory PIF action.

Short-term sPIF infusion also protects against SDM development long-term followed for 5 months post-therapy. Similarly low doses of subcutaneous sPIF injections proved effective in the same model long-term. Remarkably even after such long follow-up period post-therapy pancreatic histology mimics the islet preservation seen in ATDM. Thus, sPIF provides a long-term protection irrespective whether diabetes develops acutely or progressively over a long period of time. Thus using sPIF for early-stage TIDM management may achieve long-term protection.

The decision to use low dose sPIF in both NOD models is based on data on circulating levels of PIF that are present in pregnant women. These low levels were demonstrated to display essential multi-targeted effects, by regulating immunity, promoting embryo-decidual adhesion, regulating adaptive apoptotic processes in decidual cells and promoting trophoblast invasion [26, 27]. Further sPIF concentrations used had to vary between continuous and episodic administrations. Clinical application requires

preferably subcutaneous injections administered at the lowest dose possible. Since low-dose was effective in both ATDM and SDM indicate possible practical clinical translation of sPIF for early-stage TIDM management.

To document sPIF's induced protection against islets destruction and insulin staining preservation beyond comparing sPIF treatment to PBS control we have also analyzed the pancreas of naïve male NOD mice—non-diabetic, matched for age. This is relevant since clinical manifestations of diabetes are evident only when the number and functionality of the pancreatic islets is severely compromised and only a limited percent, $\sim$10% remains functional. We found that compared to control, PIF had a threefold increase in islet scoring; however, this was lower than found in naïve mice. This implies that remarkably long-term post-PIF therapy islets are preserved. However, the islet's score is lower, as expected when compared with that of naïve healthy mice. Whether a continuous therapy until the end of the experiment would be more effective in islet preservation is not clear at present. In contrast, insulin staining intensity in both ATDM and SDM was quasi-maximal +3 where +4 intensity is considered the highest staining achievable.

Evaluable pancreatic proteins are the ultimate gene products—were examined in SDM model following exposure to sPIF few months post-therapy. By examining both endocrine and exocrine portions of the pancreas (which are also affected in TIDM) an integrated view on sPIF effect on the target organ was possible. Beyond assessing sPIF effect versus controls pathways involved in sPIF-induced protection were also examined. Overall data reveals that sPIF affect several classes of proteins involved in TIDM pathology thereby addressing the major features of the disease. sPIF decreased pro-inflammatory proteins related to mast cells, (Cpa1) [29] and macrophages, (Chi3l3) [30]. In contrast, it increased cytokeratin 8, which blocks TNF-α-induced inflammation [31], while decreasing ferritin activated by a TNF- α related pathway [32] and pro-inflammatory elastase 3, which is increased in diabetics [33]. sPIF increased islet enzymes (PDI 2, 6, and P4H) that decrease beta-cells apoptosis [34, 35]. sPIF preserved insulin production by decreasing actin, a negative insulin regulator [36] and increasing actin remodeling, (EEF1B2) [37, 38]. sPIF also promoted insulin receptor preservation by increasing (HSP90B1) [39]. sPIF blunted activated NOD mice immunity by lowering (HNRPA2B1and RPS10 40s). In contrast, cytokeratin 18, aconitase 2, and (ALDH6A1) proteins increased, found to be elevated in DM-resistant ALR/Lt mice [40]. This indicated that the specific protective mechanisms that are operative in diabetes resistant mice are exerted by sPIF. Remarkably sPIF also preserved exocrine pancreatic function by increasing amylase 2, and lowering CTRB1 [41]. This is of relevance in diabetes since frequently, the entire pancreas in NOD model is affected, (not only islets), due to presence of organ-wide inflammation [42].

The dual holistic GeneGo pathways analysis further confirmed that sPIF-induced action involved protein translation, elongation and folding and control of cyto-skeleton filaments and cell adhesion. Pro-insulin folding in the endoplasmatic reticulum (ER) has to be of high fidelity in order to be transported to the Golgi apparatus. The demand for protein folding is increased in TIDM creating pro-insulin over accumulation and misfolding within the ER [6]. The resulting oxidative stress due to reactive oxygen species (ROS) generation leads to islet cells apoptosis and β-cells failure [43].

Notably, sPIF preserved islets function by controlling protein processing, preventing misfolding and reducing associated oxidative stress. Overall sPIF reduced those proteins that affect endocrine and exocrine pancreas function while in parallel promoted those involved in insulin expression (seen in IHC) and its receptor function. Since the whole inflamed pancreas was evaluated it did not enable to determine exactly in the case of each protein whether it was derived from the endocrine or exocrine portion of the organ. However, the correction of such a diffuse inflammation by sPIF strongly supports its protective role. The clear maintained pancreatic architecture separating endocrine and exocrine portion is a further supportive element.

In this manuscript sPIF was tested using mouse NOD models, therefore implications for therapy in humans cannot be directly asserted. However, this mouse strain has been used previously extensively in pre-clinical studies prior to human testing. While the rate of diabetes development following ATDM is very high, in SDM it is more variable and can change among studies. However, this model is recognized as the best representative of SDM development. Finally, insulin expression was not examined directly, however, maintained islet architecture combined with intense insulin staining based on the use of a specific antibody and associated proteomics supports the view that insulin was indeed preserved.

The strengths of the paper are the use of two different models that cover both the acute and insidious stages of disease and that low dose injection short term are as effective as a more invasive pump. Documentation in all studies was carried out not only by urinary or plasma glucose but also IPGTT. The length of follow-up for several months without therapy in the spontaneous model could represent several years in human disease. Insight was gained by analyzing the evaluable proteome with ranking of the pathways involved. Collectively we demonstrate that sPIF prevents both the acutely induced or innate-altered immunity present in NOD mice, permanently lowering the

risk of developing DM. sPIF-induced protection involves both exocrine and endocrine parts of the pancreas. Of note, PIF targets Kv1.3 potassium channels, which is of high relevance for TIDM therapy [26, 44]. Additional studies are needed to elucidate whether sPIF protective effect is exerted directly on the organ and whether sPIF could also reverse active TIDM. Since in diabetes islets' ability to produce insulin is only down-regulated while cells remained viable, we suggest that sPIF could reduce local inflammation allowing islets to recover, lowering insulin usage. Examination of sPIF in a clinical setting for early-stage TIDM may thus be warranted.

Methods

Peptide synthesis

Synthetic PIF peptide sPIF, (MVRIKPGSANKPSDD) or (PIFscr) (GRVDPSNKSMPKDIA) (BioIncept, LLC) was obtained by solid-phase peptide synthesis (Peptide Synthesizer, Applied Biosystems) employing 9-fluorenyl-methoxycarbonyl (Fmoc) chemistry. Final purification (>95%) was carried out by reversed-phase high-pressure liquid chromatography (HPLC) and peptide identity was verified by matrix-assisted laser desorption/ionization—time of flight (MALDI-TOF) mass spectrometry and amino acid analysis. (Biosynthesis, Inc., Lewisville, Tx).

Mice

Six-to-seven-week-old female and male NOD/LtJ (non-obese diabetic) mice were obtained from the Jackson Laboratory (Bar Harbor, ME). The animals were fed Purina chow and acidified water (pH 2.7) ad libitum, and housed under specific pathogen-free conditions with a 12 h light cycle. All procedures were conducted using facilities and protocols approved by the Animal Care and Use Committee of the Hadassah-Hebrew University School of Medicine, Jerusalem, Israel where experiments were conducted. In addition pancreatic tissue from 6 naïve NOD/LtJ male mice were obtained from Jackson Laboratory (Bar Harbor, ME).

Splenocytes preparation for adoptive-transfer experiment

Spleens from donor (diabetic) female NOD mice (16–22 weeks old, urine glucose >1000 mg/dl) were removed aseptically, minced, and washed twice with RPMI-1640 culture medium with 10% fetal calf serum. The splenocytes were resuspended in RPMI 1640 medium supplemented with 10% FCS and antibiotic, and 25×10^6 cells in 0.2 ml were injected intravenously into irradiated male NOD mice (650 Cy).

Adoptive-transfer DM NOD model (ATDM)

In the first two independent experiments, recipient irradiated (male) NOD mice were implanted subcutaneously with Alzet pumps (Model 2004, 200 µl, Durect Corp., Cupertino, CA), containing various concentrations of sPIF (0.83–2.73 mg/kg/day) or PBS for 4 weeks and then followed by urinary glucose measurements twice weekly until day 69 when a basal and 1 h following IPGTT glucose measurements were carried out. In a third experiment irradiated male mice were injected twice daily subcutaneously for 28 days at five- to tenfold lower doses of sPIF than used in the Alzet pump experiments (or PBS) and an additional group of untreated mice which were monitored weekly by urinary glucose levels (7–8 mice/group). This model realistically covers the acutely developing disease. In the fourth experiment the effect of PIF was compared with that of scrambled PIF (PIFscr) (5 mice/group). sPIF or the control peptide were injected to mice for 15 days. Development of diabetes was monitored by measuring serially plasma glucose levels.

Spontaneous DM development in NOD model (SDM)

5–6 week-old female NOD mice (at ~12 weeks start developing diabetes) were implanted with an Alzet pump containing sPIF (0.68 or 2.5 mg/kg/day), or PBS for 4 weeks, and mice were followed for development of diabetes by determining urinary glucose levels twice weekly for 21 weeks post-therapy. In a separate long-term study, ($N = 5$–6/group) mice were injected five consecutive times per week with two very low sPIF doses (0.075, 0.15 mg/kg/day) (up to 30-fold less than the previous experiment), or PBS for 16 weeks and an additional untreated control group, total ($N = 12$). Mice were followed twice weekly with urinary glucose determination for 14 weeks post-therapy. Diabetes onset was determined when >250 mg/dl urinary glucose was documented in two consecutive time periods and confirmed by measurement of blood glucose before and after IPGTT. Mice were categorized as healthy, having latent diabetes or being diabetic. This model realistically covers the spontaneously developing diabetes.

Diabetes testing

DM development was monitored by two different tests. Urinary glucose levels were tested with a test strip (Medi-Test, Combi 9, Macherey–Nagel GmbH & Co., Duren, Germany) and DM was considered to be present if

glucosuria >250 mg/dl was observed in at least two consecutive determinations. For the IPGTT test, mice were injected glucose intraperitoneally (1 gm/kg of body weight) and blood was drawn from the paraorbital plexus at 0 and 60 min after glucose administration. A plasma glucose level >200 mg/dl at the 60 min time-point measured using a glucose analyzer (Ascensia Glucometer Elite, Bayer HealthCare LLC, Tarrytown, NY), was considered positive.

Immunohistochemical insulin staining

Formalin-fixed, paraffin-embedded pancreatic tissue samples from sPIF-, PBS-treated, or Naïve mice were sectioned into 4 μm slices, mounted onto Capillary Gap Plus Slides (Fisher Scientific, Pittsburgh, PA), dried at 60°C for 1 h, deparaffinzed in xylene, and rehydrated through graded alcohol solutions to distilled water. Each section underwent 20 min of steam pretreatment using a commercial vegetable steamer (Black and Decker, Model HS 800) with 10 mmol/l, pH 6.0 citrate buffer After cooling, the slides were placed in a slide carrier and put into a Techmate 500/1000 automated immunostainer (Ventana Medical Systems, Inc., Tucson, AZ). After inhibition of endogenous peroxide activity with 3% hydrogen peroxide, the sections were incubated with normal blocking buffer for 15 min. A primary anti-insulin polyclonal antibody (guinea pig anti-insulin, diluted 1:1200, Catalog #A0564, Dako SA, Carpinteria, CA) was added for 60 min at room temperature, then the slides were washed in Tris-buffered saline (TBS), and incubated with a biotinylated secondary monoclonal antibody (goat anti-guinea pig IgG, diluted 1:400, Catalog #BA-7000, Vector Laboratories, Inc., Burlingame, CA). After incubation with ABC peroxidase (Vector Elite, Vector Laboratories) the slides were washed in TBS and then developed with the chromogen 3′-diaminobenzidine. The slides were then counterstained with a modified Mayer's hematoxylin, dehydrated, cleared, and coverslipped. Positive and negative controls were included in each staining protocol. Results were evaluated blindly by carrying out islet scoring analyzing multiple sections counting the number of islets, intact islets; partially infiltrated islets and peri-infiltrated islets; totally infiltrated islets; destroyed islets. In addition, semi-quantitative assessment of insulin staining was carried out, and analyzed using non-parametric ANOVA.

Splenocyte culture

At the end of the sPIF versus PIFscr study spleens from euthanized mice were harvested and splenocytes isolated. Cells were cultured in DMEM medium supplemented with 10% fetal bovine serum, 2 mM L-glutamine, 100 U/ml penicillin and 100 μg/ml streptomycin. Cells were cultured in duplicate at 5×10^6 cells/well in a total volume of 2 ml. Positive control wells were cultured with ConA. All wells were incubated for 3 days. After the period of incubation the supernatant was collected and frozen in −80. Cytokine concentrations in the supernatant were determined by FlowCytomix kit.

Cytokine testing

At the time of euthanizing, mouse blood samples at day 15 were collected in heparinized tubes, were separated, and the plasma collected and the mouse spleen supernatant were tested. The cytokine levels were determined by using the FlowCytomix Mouse Th1/Th2 10plex (GM-CSF, IFN-g, IL-1a, IL-2, IL-4, IL-5, IL-6, IL-10, IL-17, TNF-a) BMS820FF using the manufacturer recommendation, Bender MedSystems GmbH (Vienna, Austria).

Tissue processing

Formalin-fixed tissue blocks from three mouse pancreas tissues were randomly chosen for analysis; one from a diabetic animal, one from a healthy animal receiving sPIF at 0.075 mg/dose/day and one from a healthy animal receiving sPIF at 0.15 mg/dose/day. Five micrometer thick pancreatic tissue sections were stained with hematoxylin and eosin for standard histological analysis that confirmed the mice health status. For tissue isolation and preparation of analyzable protein, the manufacturer's recommendations were followed (Expression Pathology Inc., Gaithersburg, MD). In brief, a single 10-μm tissue section was cut from each of the three separate tissue blocks onto standard glass slides. Each slide was treated with xylene to remove paraffin and rehydrated through a series of graded ethanol solutions and distilled water. An area 8 mm^2 in size, corresponding to approximately 30,000 cells, was procured from each of the three slides by needle dissection and placed into separate standard microcentrifuge tubes. This experiment was designed to insure that tissue sampling will represent the entire organ.

Sample preparation

Collected tissues were processed with the Liquid Tissue® MS Protein Prep Kit according to manufacturer's recommendations (Expression Pathology Inc., Gaithersburg, MD). Briefly, tissue was suspended in 20 μl of Liquid Tissue® Buffer, incubated at 95°C for 90 min, and cooled on ice for 2 min. Trypsin (1 μg) was added and incubated at 37°C overnight. Each sample was heated for 5 min at 95°C to inactivate the trypsin. Total protein was measured by a micro BCA protein assay (PIERCE, Rockford, IL)

followed by addition of DTT to a final concentration of 10 mM. Each sample was then heated for 5 min at 95°C followed by storage at −20°C until LC/MS/MS analysis.

Mass spectrometric protein analysis

Mouse pancreas proteins from unstained slides from one control diabetic and two, one low and one high-dose PIF-treated mice that remained diabetes free at week 35 in the spontaneous long-term model were further analyzed. Twenty microgram of each lysate was loaded in triplicate onto a sodium dodecyl sulfate polyacrylamide gel electrophoresis (SDS-PAGE) gel (Novex 4–12%, Invitrogen, Carlsbad, CA). Each lane was excised into 10 equal slices, digested with trypsin, and analyzed by nano-liquid chromatography/mass spectrometry (nano-LC/MS/MS) on an LTQ-Orbitrap XL^{TM} tandem mass spectrometer (ThermoFisher, San Jose, CA). Production data were searched against the Mascot concatenated forward-and-reversed v3.38 International Protein Index rat database (Matrix Science Ltd., London, U.K.) and collated into non-redundant lists using Scaffold software (Proteome Software Inc., Portland, OR). Spectral counting was employed for relative quantitation, and an ANOVA followed by t-test was utilized to show significant differences.

Statistical analysis

The proportion of mice that developed diabetes was determined by using a χ^2 test. The percentage of mice that developed diabetes during the study period was evaluated using a non-parametric, area under the curve Mann–Whitney test. Glucose levels were evaluated by ANOVA, followed by unpaired *t*-test. Histological data of islet number derived from multiple section of a pancreas were analyzed by ANOVA followed by unpaired two-tailed student *t*-test, and by Mann–Whitney test in assessing insulin intensity grade. Proteome data analysis was carried out by ANOVA followed by unpaired two-tailed student *t*-test.

Proteomic pathway analysis

Pathways analysis was conducted using GeneGo's Inc systems biology analysis platform, MetaCore 6.0 that exploits a manually curated data base with experimentally validated interactions. Enrichment analysis options were used to determine the biological relevance of the collective list of proteins from the mass spectrometry results. To compare experiments, workflow were used to normalize the PIF-treated results to the control group and using several GeneGo-created ontologies, we determined the most representative canonical GeneGo maps, process networks and diseases. The results were first scored according to hypergeometric statistical evaluation and the data responsible for map or network enrichment was overlaid on top of representative pre-built GeneGo –created pathways.

Acknowledgments We thank Professor Naor, Hebrew U, Jerusalem, Israel, for donating NOD mice. We thank Kay Jenkins for analyzing the mice pancreas by IHC. sPIF is a proprietary compound (BioIncept LLC).

References

1. M.M. Lederman, J.J. Ellner, H.M. Rodman, J. Immunol. **127**, 2051–2055 (1981)
2. M. Asano, M. Toda, N. Sakaguchi, S. Sakaguchi, J. Exp. Med. **184**, 387–396 (1996)
3. B. Salomon, D.J. Lenschow, L. Rhee, N. Ashourian, B. Singh, A. Sharpe, J.A. Bluestone, Immunity **12**, 431–440 (2000)
4. D. Bresson, M. von Herrath, Drug Discov. Today Dis. Mech. **1**, 321–327 (2004)
5. J.J. Devoss, A.K. Shum, K.P. Johannes, W. Lu, A.K. Krawisz, P. Wang, T. Yang, N.P. Leclair, C. Austin, E.C. Strauss, M.S. Anderson, J. Immunol. **181**, 4072–4079 (2008)
6. D. Pitocco, F. Zaccardi, E. Di Stasio, F. Romitelli, F. Martini, G.L. Scaglione, D. Speranza, S. Santini, C. Zuppi, G. Ghirlanda, Diabetes Res. Clin. Pract. **86**(3), 173–176 (2009)
7. R.A. Ritzel, Front. Biosci. **14**, 1835–1850 (2009). Review
8. K.C. Herold, W. Hagopian, J.A. Auger, E. Poumian-Ruiz, L. Taylor, D. Donaldson, S.E. Gitelman, D.M. Harlan, D. Xu, R.A. Zivin, J.A. Bluestone, N. Engl. J. Med. **346**, 1692–1698 (2002)
9. G.S. Eisenbarth, S. Srikanta, R. Jackson, S. Rabinowe, R. Dolinar, T. Aoki, M.A. Morris, Diabetes Res. **2**, 271–276 (1985)
10. I. Raz, D. Elias, A. Avron, M. Tamir, M. Metzger, I.R. Cohen, Lancet **358**, 1749–1753 (2001)
11. M. Bitan, L. Weiss, M. Zeira, S. Reich, O. Pappo, S. Vlodavsky, S. Slavin, Diabetes Metab. Res. Rev. **24**, 413–421 (2008)
12. L. Weiss, S. Slavin, S. Reich, P. Cohen, S. Shuster, R. Stern, E. Kaganovsky, E. Okon, A.M. Rubinstein, D. Naor, Proc. Natl. Acad. Sci. USA **97**, 285–290 (2000)
13. G. Elkin, T.B. Prigozhina, S. Slavin, Prevention of TIDM in nonobese diabetic mice by non myeloablative allogenic bone marrow transplantation. Exp. Hematol. **32**, 579–584 (2004)
14. M. Koulmanda, E. Budo, S. Bonner-Weir, A. Qipo, P. Putheti, N. Degauque, H. Shi, Z. Fan, J.S. Flier, H. Auchincloss Jr., X.X. Zheng, T.B. Strom, Proc. Natl. Acad. Sci. USA **104**, 13074–13079 (2007)
15. B. Runmarker, O. Andersen, Brain **188**, 253–261 (1995)
16. A. Doria, L. Iaccarino, S. Arienti, A. Ghirardello, S. Zampieri, M.E. Rampudda, S. Cutolo, A. Tincani, S. Todesco, Reprod. Toxicol. **2**, 234–241 (2006). Review
17. C. Huang, F. Snider, J.C. Cross, Endocrinology. **150**, 1618–1626 (2009). Epub 2008 Nov 26
18. M. Ostensen, F. Forger, BMJ **328**, 915 (2004)
19. E. R. Barnea, R. Perez, P. C. Leavis, Assays for preimplantation factor and preimplantation factor peptides. USPTO 7,273,708 B2. September 2007
20. E.R. Barnea, J. Simon, S.P. Levine, C.B. Coulam, G.S. Taliadouros, P.C. Leavis, Am. J. Reprod. Immunol. **42**, 95–99 (1999)
21. E.R. Barnea, Am. J. Reprod. Immunol. **51**, 319–322 (2004)
22. E.R. Barnea, Ann. N. Y. Acad. Sci. **1110**, 602–618 (2007)
23. E.R. Barnea, S. Sharma, Prediction of implantation in ART using molecular biology, in *Contemporary Perspectives on Assisted*

Reproductive Technology, ed. by G.N. Allahbadia, R. Merchant (Reed Elsevier, India, 2007), pp. 183–194
24. E. R. Barnea, in *Signaling Between Embryo and Mother in Early Pregnancy: Basis for Development of Tolerance*. ed. by H. Carp. Recurrent Pregnancy Loss (Taylor & Francis, London) pp. 15–22
25. E. R. Barnea, D. Kirk, PIF modulated gene expression in human Peripheral Blood Mononuclear Cell (PBMC) (Homo sapiens GSE18291 [Accession]) (2009), www.ncbi.nlm.nih.gov
26. M. J. Paidas, G. Krikun, J. Huang, R. Jones, M. Romano, J. Annunziato, E. R. Barnea, Am. J. Obstet. Gynecol. **202**, 459.e1–459.e8 (2010)
27. C. Duzyj, E. R. Barnea, M. Li, S. J. Huang, G. Krikun, M. J. Paidas, *Am J Obstet Gynecol*, **203**, 402.e1–402.e4 (2010). Epub 2010 Aug 12
28. M. Jurewicz, S. Yang, A. Augello, J. G. Godwin, R. F. Moore, J. Azzi, P. Fiorina, M. Atkinson, M. H. Sayegh, R. Abdi, Diabetes (2010). Sept 2010 Ahead of print
29. R. Geoffrey, S. Jia, A.E. Kwitek, J. Woodliff, S. Ghosh, A. Lernmark, X. Wang, M.J. Hessner, J. Immunol. **177**, 7275–7286 (2006)
30. A.D. Recklies, C. White, H. Ling, Biochem. J. **365**, 119–126 (2002)
31. B. Zhong, P. Strand, D.M. Toivola, G.Z. Tao, X. Ji, H.B. Greenberg, M.B. Omary, Mol. Biol. Cell **18**, 4969–4978 (2007)
32. L.G. Xu, M. Wu, J. Hu, Z. Zhai, H.B. Shu, J. Leukoc. Biol. **72**, 410–416 (2002)
33. J. M. Fernández-Real, F. Equitani, J. M. Moreno, M. Manco, F. Ortega, W. Ricart. J. Clin. Endocrinol. Metab. (2008) Dec 30. [Epub ahead of print]
34. I.C. Gerling, S. Sudhir, N.I. Lenchik, D.R. Marshall, J. Wu, Mol. Cell. Proteomics **5**, 293–306 (2006)
35. K.S. Na, B.C. Park, M. Jang, S. Cho, H. do Lee, S. Kang, C.K. Lee, K.H. Bae, S.G. Park, Mol Cells **24**, 261–267 (2007)
36. S.S. Solomon, N. Buss, J. Shull, S. Monnier, G. Majumdar, J. Wu, C. Gerling, J. Lab. Clin. Med. **145**, 275–283 (2005)
37. D.C. Thurmond, C. Gonelle-Gispert, M. Furukawa, P.A. Halban, J.E. Pessin, Mol. Endocrinol. **17**, 732–742 (2003)
38. Y.W. Chang, J.A. Traugh, M. Li, Mol. Cell. Biol. **28**, 4549–4561 (2008)
39. R.R. Ramos, A.J. Swanson, J. Bass, Proc. Natl. Acad. Sci. **104**, 10470–10475 (2007)
40. P. Yang, M. Li, D. Guo, F. Gong, B.L. Adam, M.A. Atkinson, C.Y. Wang, Ann. N. Y. Acad. Sci. **1150**, 68–71 (2008)
41. R.M. Szmola, C. Sahin-Tóth, Proc. Natl. Acad. Sci. **104**, 11227–11232 (2007)
42. T.M. Hansner, M. Kauer, G. Gornitzka, H. Kolb, S. Martin, Exp. Clin. Endocrinol. Diab. **112**, 288–293 (2004)
43. A. E.Handel, L. Handunethi, G. C. Ebers, S. V. Ramagopalan, *Nat Rev Endocrinol.* **5**(12), 655–664 (2009). Epub 2009 Nov
44. B. H. Choi, *S.* J. Hahn, Acta Pharmacol. Sin (2010) **31**, 1031–1035